

LASER METHODS IN BIOLOGY

PACS numbers: 42.25.Fx; 87.57.Gg; 87.64.Cc
DOI: 10.1070/QE2007v037n08ABEH013611

Optical anisotropy of fibrous biological tissues: analysis of the influence of structural properties

D.A. Zimnyakov, Yu.P. Sinichkin, O.V. Ushakova

***Abstract*. The results of theoretical analysis of the optical anisotropy of multiply scattering fibrillar biological tissues based on the model of an effective anisotropic medium are compared with the experimental *in vivo* birefringence data for the rat derma obtained earlier in spectral polarisation measurements of rat skin samples in the visible region. The disordered system of parallel dielectric cylinders embedded into an isotropic dielectric medium was considered as a model medium. Simulations were performed taking into account the influence of a partial mutual disordering of the bundles of collagen and elastin fibres in derma on birefringence in samples. The theoretical optical anisotropy averaged over the spectral interval 550 – 650 nm for the model medium with parameters corresponding to the structural parameters of derma is in good agreement with the results of spectral polarisation measurements of skin samples in the corresponding wavelength range.**

Keywords: *laser diagnostics of biological tissues, polarisation spectroscopy, fibrous tissues, optical anisotropy, multiple scattering, effective medium.*

1. Introduction

Probing of biological tissues with polarised radiation in the visible and near-IR spectral regions is a promising method of medical diagnostics for determining pathological changes in the structure of biological tissues [1 – 3]. The morphological analysis of biological objects is based in some cases on illumination of a tissue region under study by linearly polarised light and recording of the two linearly polarised components of a backscattered optical signal with mutually orthogonal polarisation planes [4 – 6]. The polarisation vector of one of the detected components is selected parallel to the polarisation vector of the illuminating beam (co-polarised component of intensity $I_{||}$); another, cross-polarised component of intensity $I_{\perp}$ has the polarisation vector orthogonal to the polarisation vector of the illuminating beam.

D.A. Zimnyakov, Yu.P. Sinichkin Saratov State University, ul. Astrakhanskaya 83, 410012 Saratov, Russia; e-mail: zimnyakov@sgu.ru;
O.V. Ushakova Saratov State Technical University, ul. Politekhnicheskaya 77, 410071 Saratov, Russia

Received 4 May 2007
Kvantovaya Elektronika **37** (8) 777 – 783 (2007)
Translated by M.N. Sapozhnikov

The multiple scattering of polarised light in random media, to which most of biological tissues belong, leads to its partial or complete depolarisation (depending on the tissue structure and the probe radiation wavelength). In this case, the cross-polarised component, which is often called the depolarised component, is mainly formed due to multiple scattering of light penetrating into a medium being probed to the depth exceeding the transport length l^* (l^* is the characteristic distance in a multiply scattering medium at which the directed propagation regime passes to the diffusion regime [7]). At the same time, the backscattered co-polarised component is an incoherent mixture of diffusion radiation scattered in deep tissue layers and few-order scattered radiation coming mainly from surface layers. Therefore, the difference of the intensities of the co-polarised and cross-polarised components $\Delta I_{||,\perp} = I_{||} - I_{\perp}$ gives the optical signal formed predominantly by single-order scattering in surface tissue layers.

Such an approach was used, for example, in the method of polarisation spectroscopy of biological tissues [8, 9] to estimate the average size and refractive index of the nuclei of epithelial cells by analysing fluctuations in the difference spectra $\Delta I_{||,\perp}$ caused by Mie resonances observed upon single-order scattering of probe radiation by the nuclei. In turn this allows one to observe pathologies in the morphology of cellular layers at the displasia stage and the early cancer stage. The normalised difference signal $P_{\mathrm{L}} = \Delta I_{||,\perp}/(I_{||} + I_{\perp})$, or the residual linear polarisation of scattered radiation was used in papers [10 – 12] to obtain contrast images of the tissue structure at depths of the order of $(1-3)l^*$ for morphological diagnostics and visualisation of pathologies. The use of broadband probe radiation sources and partial spectral selection of detected scattered radiation (for example, with the help of interference filters or, more roughly, by analysing separately the R, G, and B components of colour polarisation images) offers additional possibilities. The main factors affecting the value of P_{L} upon the spectral selection of scattered radiation are:

(i) The anisotropy parameter g of a medium being probed [for media with small g ($g \leqslant 0.3$), consisting mainly of scatterers with the characteristic size $d \ll \lambda$, where λ is the probe radiation wavelength, the residual linear polarisation of backscattered radiation typically exceeds that for media with $g \geqslant 0.8$ [13 – 15]);

(ii) the absorption coefficient of the medium, which is determined by the content of chromophores (for example, haemoglobin) in it [16, 17].

The increase of the absorption coefficient in some spectral regions (for haemoglobin, between 545 and

575 nm) leads to the suppression of multiply scattered components characterised by large optical paths in the medium being probed, resulting in the reduction of the cross-polarised component in the detected optical signal compared to the co-polarised component. In particular, the residual linear polarisation of scattered radiation increases with increasing the microcirculation of blood in surface tissue layers (for example, due to local inflammatory processes), which is observed upon polarisation visualisation of skin burns [18].

The macroscopic anisotropy of morphological and, correspondingly, optical properties of some biological tissues (for example, muscular tissue, sinews, derma) caused by their fibrillar structure with partially oriented close-packed fibres is specifically manifested in the polarisation diagnostics and visualisation of tissues. For example, in the case of *in vivo* polarisation video reflectometry of the animal and human derma with the use of focused probe laser radiation beams [19], the equal-intensity lines ($I_{||} + I_{\perp}$) in the images of the surface of samples obtained in diffusely reflected light have the characteristic elliptic shape. The eccentricity of the equal-intensity ellipses depends on the distance between the probed region and the region of coupling of the probe radiation into a sample. At distances considerably exceeding the maximal value of the transport length of a sample under study, the ratio of the major and minor axes of ellipses is determined by the parameter $(\mu'_{s||}/\mu'_{s\perp})^{1/2}$. Here, $\mu'_{s||}$ and $\mu'_{s\perp}$ are the transport scattering coefficients [7] of probe radiation propagating in a medium along fibres and perpendicular to them, respectively. The spatial distributions of polarisation parameters of detected scattered radiation (in particular, P_L) also have anisotropy.

Note that for principal directions in a medium being probed, which are determined by the predominant orientation of fibres forming the structure, the structural anisotropy of such multiply scattering media should be manifested not only in different values of the transport parameters of the medium (the transport scattering coefficient μ'_s, the scattering coefficient μ_s, and the anisotropy parameter g). Another characteristic property of fibrous tissues with partially oriented fibres is birefringence, which is manifested at macroscopic scales exceeding considerably the transport length of the medium. When a detected optical signal contains the unscattered ('ballistic') and (or) few-order scattered components (for example, upon probing optically thin tissue layers by detecting small-angle forward-scattered radiation or in the study of the structure of surface tissue layer by the method of optical coherence tomography), the analysis of polarisation parameters of detected radiation should take into account not only depolarisation caused by multiple scattering of the probe linearly polarised radiation in the medium but also the transformation of polarisation (in the general case, from linear to elliptic) for the unscattered and few-order scattered components. This opens up new possibilities in studying pathologies of the fibrillar structure of tissues [20]. For example, the method of polarisation-sensitive optical coherence tomography was used in papers [21, 22] to analyse the depth of derma burns producing the partial or complete denaturation of collagen fibres. In this case, the burn depth is estimated by the phase shift between the orthogonally polarised components of detected radiation, which is measured for the specified probe depth of the burnt tissue region and is determined by the optical anisotropy $\Delta n = n_{||} - n_{\perp}$.

We studied earlier [23] the polarisation properties of *in vitro* rat skin samples in the visible region from 500 to 700 nm by using spectral polarisation measurements in transmitted light. The absolute value $|\Delta n|$ of optical anisotropy averaged over the 550 – 650-nm wavelength region was measured. The measurements showed that the dispersion of birefringence $\mathrm{d}(\Delta n)/\mathrm{d}\lambda$ of the skin derma in the spectral region studied was small. The aim of the present paper is to interpret the experimental data obtained earlier by using the model of an effective medium taking into account the optical anisotropy of multiply scattering media with a partially oriented fibrillar structure.

2. Model of an anisotropic effective medium

The influence of the morphological parameters of multiply scattering random media with a fibrillar structure was analysed by using a model scattering system consisting of parallel dielectric cylinders of radius R_{cyl} with the refractive index n_{cyl} and the volume fraction f. The cylinders are randomly distributed in a dielectric medium with the refractive index n_{bk}. The effective refractive indices $n_{eff||}$ and $n_{eff\perp}$ for such a model medium are calculated in cases when the electric-field vector of a linearly polarised monochromatic electromagnetic wave with the unit amplitude propagating in the medium is oriented parallel or perpendicular to the axes of cylinders. The macroscopic optical anisotropy is $\Delta n = n_{eff||} - n_{eff\perp}$. We calculated $n_{eff||}$ and $n_{eff\perp}$ by the method proposed in papers [24, 25], which uses the criterion of the equality of the energy of the electromagnetic field in the volume of a medium occupied by a model scattering centre to the field energy in the equivalent volume of the effective spatially homogeneous medium with refractive indices $n_{eff||}$ or $n_{eff\perp}$. As a model scattering centre, a dielectric cylinder of radius R_{cyl} with the refractive index n_{cyl} in a cylindrical dielectric shell with the refractive index n_{bk} is considered. The shell radius $R_{coat} = R_{cyl}/\sqrt{f}$ is determined by the volume fraction of cylinders in the model medium.

The conditions of the equality of the energies of the electromagnetic field in the volume occupied by a model scattering centre $[W_{||}(n_{cyl}, n_{bk}, n_{eff||}),\ W_{\perp}(n_{cyl}, n_{bk}, n_{eff\perp})]$ and in the equivalent volume of a spatially homogeneous medium $[W_0(n_{eff||}),\ W_0(n_{eff\perp})]$ in the case of a propagating plane monochromatic linearly polarised wave have the form (per unit length of a cylindrical scattering centre)

$$
\begin{aligned}
W_{||,\perp}(n_{cyl}, n_{bk}, n_{eff||,\perp}) &= \int_0^{R_{coat}} \mathrm{d}^2 r \{[\varepsilon_0 n^2(r)|\boldsymbol{E}_{||,\perp}(r)|^2 \\
&\quad + \mu_0 |\boldsymbol{H}_{||,\perp}(r)|^2]/2\}, \\
W_0(n_{eff||,\perp}) &= \int_0^{R_{coat}} \mathrm{d}^2 r \{[\varepsilon_0 n^2_{eff||,\perp}|\boldsymbol{E}_{||,\perp}(r)|^2 \\
&\quad + \mu_0 |\boldsymbol{H}_{||,\perp}(r)|^2]/2\}, \\
W_{||}(n_{cyl}, n_{bk}, n_{eff||}) &= W_0(n_{eff||}), \\
W_{\perp}(n_{cyl}, n_{bk}, n_{eff\perp}) &= W_0(n_{eff\perp}),
\end{aligned}
\tag{1}
$$

where

$$n(r) = \begin{cases} n_{\rm cyl}, & 0 \leqslant r \leqslant R_{\rm cyl}, \\ n_{\rm bk}, & R_{\rm cyl} < r \leqslant R_{\rm coat}; \end{cases}$$

ε_0 and μ_0 are the permittivity and permeability of the medium; $\boldsymbol{E}_{||,\perp}(r)$ and $\boldsymbol{H}_{||,\perp}(r)$ are the strengths of the electric and magnetic components of the electromagnetic field of a light wave for different orientations of the electric component with respect to the axes of cylinders.

The values of $\boldsymbol{E}_{||,\perp}(r)$ and $\boldsymbol{H}_{||,\perp}(r)$ are calculated by expanding them in the Bessel and Neumann series for a spatial region inside a dielectric cylinder ($0 \leqslant r \leqslant R_{\rm cyl}$), in the dielectric shell ($R_{\rm cyl} < r \leqslant R_{\rm coat}$), and outside the model scattering centre ($r > R_{\rm coat}$) [26, 27]. The expansion coefficients are calculated by using the boundary conditions for the tangential components of the electric and magnetic field strengths at the cylinder–shell and shell–environment interfaces. The environment is simulated by the effective medium with the refractive index $n_{\rm eff||}$ or $n_{\rm eff\perp}$. The values of $n_{\rm eff||}$ and $n_{\rm eff\perp}$, at which conditions (1) are fulfilled for the specified orientation of the electric field vector with respect to the axes of cylinders and for the specified values of $n_{\rm cyl}$, $n_{\rm bk}$, $R_{\rm cyl}$ and f, are used as the effective refractive indices of the probed medium for the specified orientation of the electric field vector of the propagating wave.

Figure 1, illustrating the method of determining $n_{\rm eff||}$ and $n_{\rm eff\perp}$ for $\lambda = 600$ nm, shows the dependences of the average energy density $W_{||}(n_{\rm cyl}, n_{\rm bk}, n_{\rm eff||})/\pi R_{\rm coat}^2$, $W_{\perp}(n_{\rm cyl}, n_{\rm bk}, n_{\rm eff\perp})/\pi R_{\rm coat}^2$, and $W_0(n_{\rm eff||,\perp})/\pi R_{\rm coat}^2$ in the volume of the effective scattering centre on $n_{\rm eff||,\perp}$ for $n_{\rm cyl} = 1.50$, $n_{\rm bk} = 1.30$, $R_{\rm cyl} = 50$ and $f = 0.6$ ($R_{\rm cyl}$ and f are taken equal to the radius and the volume fraction of collagen fibres, respectively, which are typical for many partially ordered fibrous tissues (see, for example, [28, 29]).

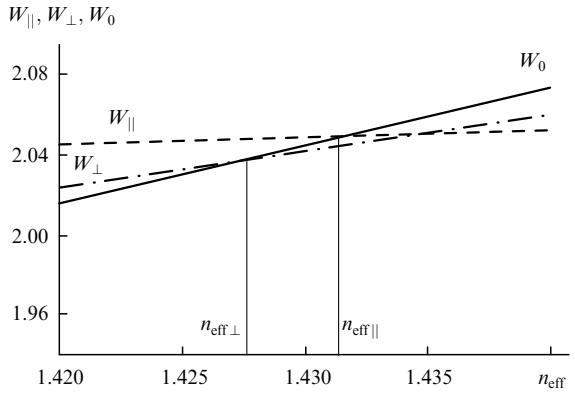

Figure 1. Graphical representation of the method for determining $n_{\rm eff||}$ and $n_{\rm eff\perp}$ for $n_{\rm cyl} = 1.50$, $n_{\rm bk} = 1.30$, $R_{\rm cyl} = 50$ nm, $f = 0.6$, and $\lambda = 600$ nm; $W_{||}(n_{\rm cyl}, n_{\rm bk}, n_{\rm eff||})$, $W_{\perp}(n_{\rm cyl}, n_{\rm bk}, n_{\rm eff\perp})$, $W_0(n_{\rm eff||,\perp})$ are normalised to the geometrical cross section $\pi R_{\rm coat}^2$ of dielectric cylinders.

Analysis of the dependence of the optical anisotropy Δn of the model medium on the excitation wavelength showed that the asymptotic values of $n_{\rm eff||}$ and $n_{\rm eff\perp}$ in the low-frequency limit ($\lambda \to \infty$) are independent of the diffraction parameter $2\pi R_{\rm cyl}/\lambda$ of scattering centres and are determined only by the values of $n_{\rm cyl}$, $n_{\rm bk}$ and f. It was shown in [25] that in the case of $\lambda \gg R_{\rm cyl}$, the effective value $\varepsilon_{\rm eff\perp}$ of the relative permittivity of the disordered system of close-packed parallel dielectric cylinders with a high relative permittivity in air ($\varepsilon_{\rm cyl} = 9$, $\varepsilon_{\rm bk} \approx 1$) for a linearly polarised electromagnetic wave with the electric field vector oriented perpendicular to the axes of cylinders can be obtained by averaging the permittivity $\varepsilon_{\rm cyl}$ of cylinders and of their environment ($\varepsilon_{\rm bk}$) over the volume: $\varepsilon_{\rm eff\perp} = \varepsilon_{\rm cyl} f + \varepsilon_{\rm bk}(1-f)$. In the case of the parallel orientation of the electric field vector with respect to the axes of cylinders, the value of $\varepsilon_{\rm eff||}$ in the low-frequency limit can be calculated by using the Maxwell–Garnet model [27]:

$$\varepsilon_{\rm eff||} = \varepsilon_{\rm bk}\left(1 + \frac{2\alpha f}{1-\alpha f}\right), \tag{2}$$

where $\alpha = (\varepsilon_{\rm cyl} - \varepsilon_{\rm bk})/(\varepsilon_{\rm cyl} + \varepsilon_{\rm bk})$ is the polarisability of scattering centres (dielectric cylinders). We found that a similar relation is also valid for close-packed media based on the so-called optically soft cylindrical scattering centres characterised by low polarisabilities ($\alpha \ll 1$). Thus, the optical anisotropy of the model medium under study in the low-frequency limit ($\lambda \to \infty$) can be written in the approximate form

$$\Delta n = \sqrt{\varepsilon_{\rm eff||}} - \sqrt{\varepsilon_{\rm eff\perp}} \approx \left[\varepsilon_{\rm bk}\left(1 + \frac{2\alpha f}{1-\alpha f}\right)\right]^{1/2} - \left[\varepsilon_{\rm bk}(1-f) + \varepsilon_{\rm cyl} f\right]^{1/2}. \tag{3}$$

Note that Hemenger proposed [30, 31] the different expression: $\Delta n \approx f(1-f)(n_{\rm cyl} - n_{\rm bk})^2/[f n_{\rm cyl} + (1-f) n_{\rm bk}]$ for the optical anisotropy of a system of dielectric cylinders in the Rayleigh limit $2\pi R_{\rm cyl}/\lambda \to 0$. The values of Δn calculated from this expression and expression (3) for optically soft cylindrical scatterers $[(n_{\rm cyl} - n_{\rm bk})/n_{\rm cyl} \ll 1]$ in the interval $0.5 \leqslant f \leqslant 0.7$ differ by no more than 15%, the Hemenger expression predicting lower values of Δn compared to (3).

As the diffraction parameter $2\pi R_{\rm cyl}/\lambda$ increases, the value of Δn changes nonmonotonically (Fig. 2). This is explained by the different dependences of

$$\frac{W_{||}(n_{\rm cyl}, n_{\rm bk}, n_{\rm eff||})}{\pi R_{\rm coat}^2} \text{ and } \frac{W_{\perp}(n_{\rm cyl}, n_{\rm bk}, n_{\rm eff\perp})}{\pi R_{\rm coat}^2}$$

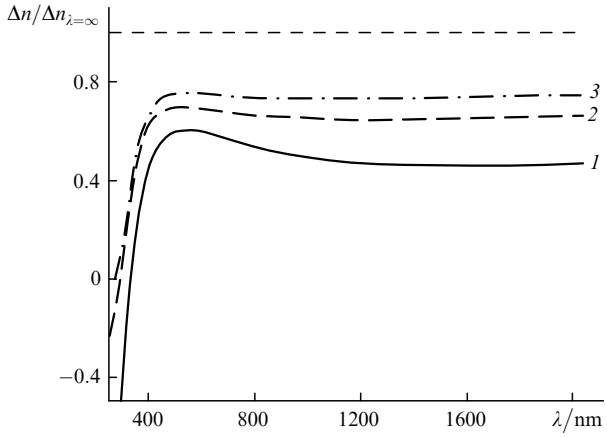

Figure 2. Normalised values of Δn for a disordered system of close-packed parallel dielectric cylinders ($R_{\rm cyl} = 50$ nm, $f = 0.6$) as functions of the probe radiation wavelength for $n_{\rm cyl} = 1.5$, $n_{\rm bk} = 1.3$ (*1*), $n_{\rm cyl} = 1.6$, $n_{\rm bk} = 1.2$ (*2*) and $n_{\rm cyl} = 1.7$, $n_{\rm bk} = 1.1$ (*3*).

on λ during the interaction of the s- and p-polarised electromagnetic waves with effective scattering centres. Figure 2 resents the dependences of the normalised values of Δn on the probe radiation wavelength for close-packed systems of cylinders with different n_{cyl} and n_{bk}; the value of Δn in the low-frequency limit calculated from (3) is used for normalisation.

Note that in the case of interaction of linearly polarised radiation with singly scattering disordered systems of anisotropic particles, the birefringence of such scattering media is controlled by the parameter ξ, which is proportional to the square of the wavelength and the imaginary part of the difference of sums of the diagonal elements of the amplitude scattering matrices of anisotropic scatterers for the zero scattering angle: $\Delta n \propto \xi = \lambda^2 \mathrm{Im}[\sum S_1(0) - \sum S_2(0)]$, where summation is performed over all scattering particles contained in the unit volume of the medium [26]. The parameter ξ for disordered systems of parallel dielectric cylinders can be written in the form

$$\xi = \lambda^2 \mathrm{Im}\left[\sum_{n=-\infty}^{n=\infty} \frac{mJ_n'(y)J_n(x) - J_n(y)J_n'(x)}{mJ_n'(y)H_n(x) - J_n(y)H_n'(x)} \right.$$

$$\left. - \sum_{n=-\infty}^{n=\infty} \frac{J_n'(y)J_n(x) - mJ_n(y)J_n'(x)}{J_n'(y)H_n(x) - mJ_n(y)H_n'(x)} \right], \qquad (4)$$

where J_n and H_n are the nth-order Bessel and Hankel functions; m is the relative refractive index of the cylinder material; $y = 2\pi m R_{cyl}/\lambda$; $x = 2\pi R_{cyl}/\lambda$. Analysis of expression (4) shows that the nonmonotonic behaviour of Δn and the change in its sign with increasing the diffraction parameter x is also manifested in the case of single-order scattering, i.e. it is a fundamental property of systems of nonabsorbing cylindrical scatterers. The single-order scattering model also predicts that $\Delta n = \mathrm{const}$ for $x \to 0$ and $|\Delta n|$ asymptotically tends to zero for $x \to \infty$. At the same time, some specific features of the dependences $\Delta n(x)/\Delta n_{\lambda=\infty}$ obtained within the framework of the effective anisotropic medium should be pointed out. In particular, the characteristic value of x corresponding to the change of the anisotropy sign in the region of large values of the diffraction parameter of scattering centres in the model of a multiply scattering medium is smaller than that predicted by the single-order scattering model [expression (4)]. For $x \to 0$, the dependence slowly saturates by tending to an asymptotic value determined by expression (3), which is accompanied by aperiodic variations with increasing the wavelength; the amplitude of these variations increases with decreasing the contrast $(n_{cyl} - n_{bk})/n_{cyl}$ of the refractive indices of cylinders and environment.

These properties are tentatively caused by cooperative effects upon multiple scattering of electromagnetic waves by ensembles of closely spaced scattering centres. Such effects are taken into account to a certain degree within the framework of the anisotropic medium model by introducing effective scattering centres (cylinders in shells). The increase in aperiodic variations of the dependences of the optical anisotropy for the model medium with decreasing $(n_{cyl} - n_{bk})$ in the case of a small diffraction parameter of scattering centres (Fig. 2) is caused by the resonances of the electromagnetic field in the effective scattering centre consisting of a cylinder and a shell with close refractive indices. It can be expected that in real multiply scattering media consisting of polydisperse scatterers such oscillations will be suppressed.

3. Influence of the orientation factor on the optical anisotropy of fibrillar media

Most of the real multiply scattering media with the fibrillar structure are characterised by a partial or complete disordering of structuring elements (fibres) with respect to a selected direction in the medium. Analysis of the data in the literature on the structure of fibrous biological tissues with partially oriented fibres (in particular, derma [28, 29]) shows that, as a rule, structuring elements (collagen or elastin fibres) are combined in groups (bundles) with the minimal mutual disordering of fibre axes; at the same time, the axes of different bundles are considerably disordered.

We analysed the influence of the orientation factor on the optical anisotropy of fibrillar media consisting of partially oriented groups of dielectric fibres by using a multilayer model of an anisotropic medium consisting of parallel anisotropic layers with the specified values of Δn and the random orientation of optical axes with respect to their predominant direction. The degree of mutual disordering of the optical axes of layers was described by the root-mean-square value δ_φ of the disordering angles of optical axes with respect to the predominant direction. We simulated the propagation of a plane linearly polarised monochromatic light wave along the normal to the boundary of layers in such a model medium with the specified values of Δn, thickness L, and the number k of layers. The direction of the predominant orientation of the optical axes of layers made an angle 45° with the polarisation plane of probe radiation.

The angle φ of deviation from the predominant direction for each of the layers was selected randomly in simulations in accordance with the simulated distribution of φ (uniform or Gaussian with the specified values of δ_φ). We studied the wavelength dependences of the intensity of the co- and cross-polarised components of radiation transmitted through the medium. The intensities were averaged over an ensemble of 1000 statistically independent values obtained in each simulation cycle with the values φ_1, φ_2, ..., φ_k selected randomly. This allowed us to take into account to a certain degree the difference in the orientation of fibre bundles not only over the depth but also in the transverse direction. The effective values Δn_{eff} of the optical anisotropy of the medium for the specified values of Δn, N and δ_φ were determined from the wavelengths corresponding to the position of the interference maxima of the adjacent orders in the dependences $I_{||}(\lambda)$ and $I_\perp(\lambda)$ obtained in simulations.

The obtained results are presented in Fig. 3 in the form of the dependence of Δn_{eff} on δ_φ for the specified optical anisotropy of a layer ($\Delta n = 1.0 \times 10^{-4}$). These dependences Δn_{eff} for other values of Δn (in the range from $5 \times 10^{-5} - 4 \times 10^{-4}$) are similar. We found that for a large number of layers ($k \geqslant 10 - 15$), the value of $\Delta n_{eff}(\delta_\varphi)$ is virtually independent of k and the number of statistically independent quantities $I_{||}(\lambda), I_\perp(\lambda)$ obtained for different sets $\varphi_1, \varphi_2, \ldots, \varphi_k$. We also found that the distribution of φ (uniform or Gaussian) for the same δ_φ weakly affects the dependences $\Delta n_{eff}(\delta_\varphi)$ obtained in simulations (Fig. 3).

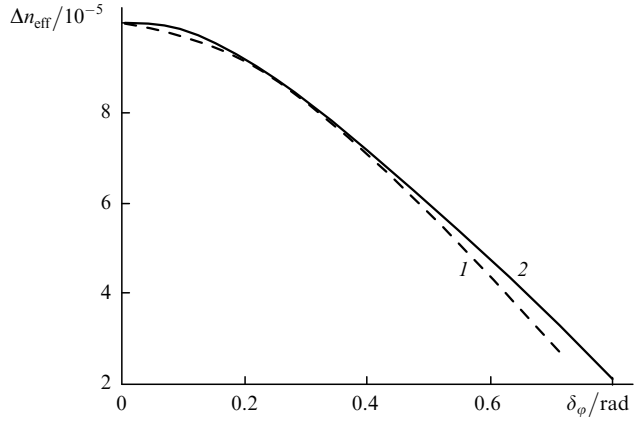

Figure 3. Dependences $\Delta n_{\rm eff}(\delta_\varphi)$ for a model 'polycrystalline' medium consisting of the fragments of anisotropic layers ($\Delta n = 1.0 \times 10^{-4}$) with partially disordered local optical axes: (*1*) the uniform distribution of the angles of deviation of local optical axes from the predominant direction and (*2*) the Gaussian distribution of deviation angles.

4. Birefringence of *in vitro* derma: the interpretation of experimental data [23] based on simulations

As mentioned above, the spectral polarisation analysis of rat skin samples *in vitro* in the transmitted light (500 – 700 nm) revealed the optical anisotropy with $|\Delta n| \approx (2.3 \pm 0.2) \times 10^{-4}$ (in the wavelength range from 550 to 650 nm), which is probably caused by a partial orientation ordering of the main structuring elements of derma – collagen and elastin fibres [23]. The estimates of Δn made for different probe radiation wavelengths showed that the dispersion of birefringence $\mathrm{d}(\Delta n)/\mathrm{d}\lambda$ of derma samples in the spectral range 550 – 650 nm was small (the difference between the values of $|\Delta n|$ at the boundaries of this spectral range does not exceed the measurement error). Analysis of the morphological data for the animal and human derma [28, 29] shows that the typical diameters of collagen and elastin fibres in derma are 50 – 100 nm (taking into account age variations and positions of skin regions used in derma samples). The average volume fraction of collagen fibres in derma is approximately 0.6 – 0.7.

Figure 4a presents a series of arbitrarily selected fragments of the electron microscope images of the human derma [23] illustrating the degree of the orientation ordering of collagen fibres grouped in bundles in derma. The sampling statistical analysis of the distribution of the deviation angles of fibre axes with respect to the specified direction performed for 100 fragments (the corresponding histogram is presented in Fig. 4b) gave the characteristic value of δ_φ for the human derma equal to $\sim 30^\circ$ (~ 0.52 rad).

Figure 5 presents the dependence of the optical anisotropy parameter Δn on the probe radiation wavelength in the range from 475 to 650 nm calculated in the model of the effective anisotropic medium for the disordered polydispersion system of parallel dielectric cylinders with $n_{\rm cyl} = 1.46$ embedded into a dielectric medium with $n_{\rm bk} = 1.37$. These values correspond to the typical refractive indices in the visible region for collagen and polysaccharides (base substance in which collagen fibres are located which form the structure of some fibrous tissues of humans and animals). The values of $n_{\rm eff\,||}$ and $n_{\rm eff\,\perp}$ were calculated by assuming

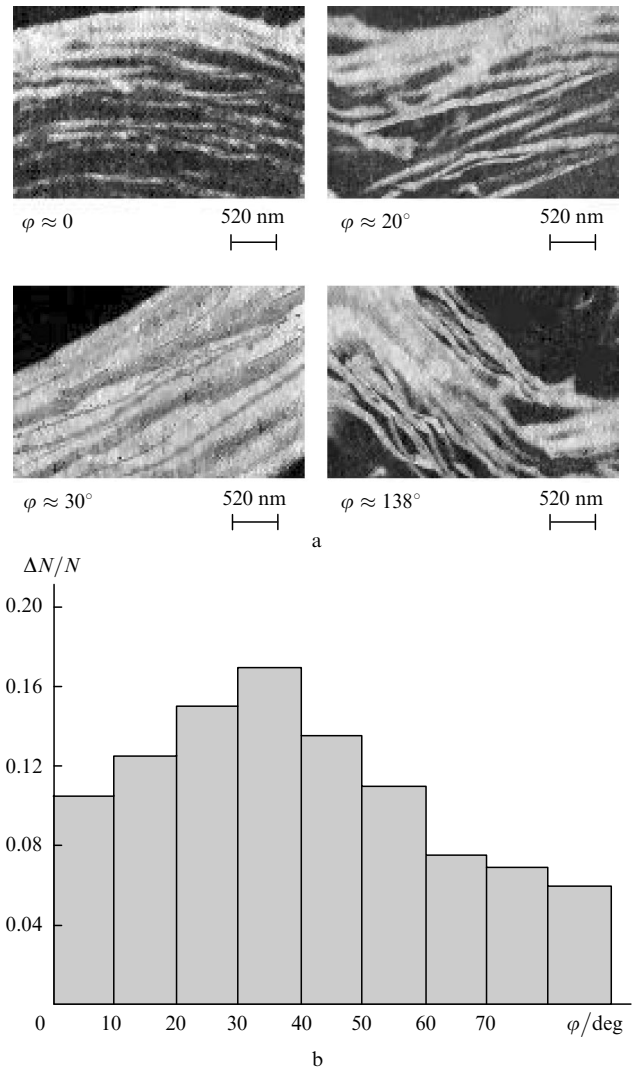

Figure 4. Examples of randomly selected fragments of the electron-microscope image of the human skin derma [29] (a) and the histogram of the angles of deviation of fibres in derma from the predominant direction of fibre axes obtained from the statistical analysis of the electron-microscopic image (b). The histogram is constructed taking into account the identity of polarisation properties of structural fragments with deviation angles φ and $\pi - \varphi$ measured in experiments.

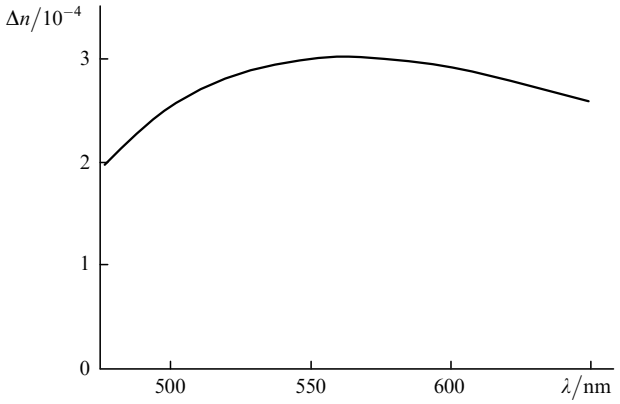

Figure 5. Averaged dependences $\Delta n(\lambda)$ calculated for systems of dielectric cylinders with the values of $R_{\rm cyl}$ uniformly distributed in the interval 35 – 65 nm. The wavelength interval corresponds to the probe radiation wavelength range used in experiments [23]; the parameters $n_{\rm cyl}$, $n_{\rm bk}$ and f have values typical for collagen fibres in derma.

that the diameter of cylinders is uniformly distributed in the interval from 80 to 120 nm and $f = 0.6$ (as mentioned above, these values correspond to typical morphological parameters characterising the fibrillar structure of derma).

The value of Δn for the dependence in Fig. 5 averaged over the 550–650-nm wavelength range is approximately 2.87×10^{-4} and well agrees with the optical anisotropy obtained in experiments with derma samples *in vitro*. Note that the dispersion Δn is relatively small in this spectral range. As mentioned above, experimental data obtained for rat skin samples demonstrate the weak dispersion of the derma birefringence in the long-wavelength region of the visible range. A drastic decrease in Δn for the model scattering system in the short-wavelength region of the visible range ($\lambda < 500$ nm) followed by a change in the optical anisotropy sign is caused, according to the theory of scattering for dielectric cylinders, by differences in the conditions of the appearance of the Mie resonances upon scattering of the s- and p-polarised waves [26, 27] by effective scattering centres for the diffraction parameter $x \geqslant 1$.

Note that this effect will be masked in the spectral polarisation measurements of fibrous tissues by the properties of spectral dependences of $n_{\mathrm{eff}\,||}$ and $n_{\mathrm{eff}\,\perp}$, caused by a strong absorption of the probe radiation by tissues in the short-wavelength region of the visible range and near-UV region. A decrease in Δn in the case of the model scattering system (for $\lambda > 600$ nm) is explained by the oscillating dependence (with a large period in λ) of the optical anisotropy of the model medium on the probe radiation wavelength, which tends asymptotically to expression (3). It can be expected that such oscillations will be suppressed in real polydispersion fibrous scattering media with partially disordered scattering centres.

According to the results of analysis of the influence of the orientation factor on the optical anisotropy of the model anisotropic medium (see Fig. 3) for the system of partially disordered dielectric cylinders with $\delta_\varphi \approx 0.52$ rad, it can be expected that Δn will be approximately smaller by a factor of 1.6 than that for a scattering system with $\delta_\varphi = 0$. At the same time, the polarisation microscopic analysis of rat skin samples performed in [23] (maps of the orientation of local slow axes are presented in Fig. 6 in [23]) demonstrates a high orientation ordering of the local optical axes of derma fragments at the spatial scale of 50 μm–1 mm (in particular, the root-mean-square of variations in the orientation of the slow optical axis over a sample region of area ~ 1 mm^2 does not exceed 7.5°, which is considerably lower than the value of δ_φ obtained from the electron-microscope images of the human skin derma, see Fig. 4). Such a difference in the values of the orientation parameter determined by different methods is tentatively caused by the influence of a number of factors. These are morphological differences of samples, the dependence of the orientation parameter on the position of skin sampling region, a considerable difference between the sizes of skin regions used to estimate δ_φ from electron-microscopic and polarisation-microscopic images. Thus, the value of Δn for the model medium under study can be estimated from the inequalities $1.7 \times 10^{-4} \leqslant \Delta n \leqslant 2.7 \times 10^{-4}$ (the lower and upper boundaries of the interval are the values of δ_φ obtained from analysis of electron-microscope and polarisation-microscope images, respectively), which is in good agreement with the values obtained earlier in spectral polarisation *in vitro* measurements of rat derma samples [23].

5. Conclusions

Despite a number of simplifying assumptions (the absence of probe radiation absorption in a model medium, the uniform spatial distribution of cylindrical scatterers, etc.), the model of the effective anisotropic medium considered in the paper gives quantitative estimates of Δn, which are in agreement with spectral polarisation measurements of fibrous tissues (*in vitro* rat skin samples). The method developed in the paper can be also used to interpret the results of studies of multiply scattering macroscopically anisotropic media by other optical diffusion methods, in particular, laser polarisation video reflectometry [19] of various fibrillar media with a partially oriented fibrillar structure. In this case, the difference in the values of $n_{\mathrm{eff}\,||}$ and $n_{\mathrm{eff}\,\perp}$ can considerably affect the reflectivity of the probed medium–free space boundary for different orientations of the polarisation plane of the focused probe laser beam with respect to the predominant orientation of fibres in the medium.

Acknowledgements. This work was supported by the Russian Foundation for Basic Research (Grant No. 07-02-01467a) and a 'Mezooptik' grant of AFGIR and the Ministry of Education of the Russian Federation [Analytic departmental program 'Development of the Scientific Potential of the Higher School (2006–2008)', project code RNP.2.1.4473].

References

1. Wang L.V., Cote' G.L., Jacques S.L. *J. Biomed. Opt.*, **7**, 278 (2002).
2. Jiao S., Gao G., Wang L.V. *Appl. Opt.*, **39**, 6318 (2000).
3. Tuchin V.V., Wang L.V., Zimnyakov D.A. *Optical Polarization in Biomedical Applications* (Berlin, Heidelberg: Springer-Verlag, 2006).
4. Anderson R.R. *Arch. Dermatol.*, **127**, 1000 (1991).
5. Jacques S.L., Roman J.R., Lee K. *Lasers Surg. Med.*, **26**, 119 (2000).
6. Jacques S.L., Ramella-Roman J.C., Lee K. *J. Biomed. Opt.*, **7**, 329 (2002).
7. Ishimaru A. *Wave Propagation and Scattering in Random Media* (New York: Academic Press, 1978; Moscow: Mir, 1981) Vols 1 and 2.
8. Myakov A., Nieman L., Wicky L., Utzinger U., Richards-Kortum R., Sokolov K. *J. Biomed. Opt.*, **7**, 388 (2002).
9. Sokolov K., Drezek R., Gossagee K., Richards-Kortum R. *Opt. Express*, **5**, 302 (1999).
10. Tyo J.S. *J. Opt. Soc. Am. A*, **17**, 1 (2000).
11. Zimnyakov D.A., Sinichkin Yu.P. *J. Opt. A: Pure Appl. Opt.*, **2**, 200 (2000).
12. Sinichkin Yu.P., Zimnyakov D.A., Agafonov D.N., Kuznetsova L.V. *Opt. Spektr.*, **93**, 99 (2002).
13. Dogariu A., Kutsche C., Likamwa P., Boreman G., Moudgil B. *Opt. Lett.*, **22**, 285 (1997).
14. Zimnyakov D.A., Sinickin Yu.P., Zakharov P.V., Agafonov D.N. *Waves Random Media*, **11**, 395 (2001).
15. Zimnyakov D.A., Sinichkin Yu.P. *Opt. Spektrosk.*, **91**, 113 (2001).
16. Zimnyakov D.A., Sinichkin Yu.P., Kiseleva I.V., Agafonov D.N. *Opt. Spektrosk.*, **92**, 848 (2002).
17. Zimnyakov D.A. *Waves Random Media*, **10**, 417 (2000).
18. Zimnyakov D.A., Sinichkin Yu.P., Tuchin V.V. *Izv. Vyssh. Uchebn. Zaved., Ser. Radiofiz.*, (10-11), 957 (2004).

19. Sviridov A., Chernomordik V., Hassan M., Russo A., Eidsath A., Smith P., Gandjbakhche A.H. *J. Biomed. Opt*., **10**, 014012 (2005).
20. Yao G., Wang L.V. *Opt. Lett*., **24**, 537 (1999).
21. Park B.H., Saxer C.E., Srinivas S.M., Nelson J.S., de Boer J.F. *J. Biomed. Opt*., **6**, 474 (2001).
22. Srinivas S.M., de Boer J.F., Park B.H., Keikhanzadeh K., Huang H., Zhang J., Jung W.Q., Chen Z., Nelson J.S. *J. Biomed. Opt*., **9**, 207 (2004).
23. Sinichkin Yu.P., Zimnyakov D.A., Yakovlev D.A., Ovchinnikova I.A., Spivak A.V., Ushakova O.V. *Opt. Spektrosk*., **101**, 851 (2006).
24. Busch K., Soukoulis C.M. *Phys. Rev. B*, **54**, 893 (1996).
25. Kirchner A., Busch K., Soukoulis C.M. *Phys. Rev. B*, **57**, 277 (1998).
26. van de Hulst H.C. *Light Scattering by Small Particles* (New York: Wiley, 1957; Moscow: IL, 1961).
27. Bohren C.F., Huffman D.R. *Absorption and Scattering of Light by Small Particles* (New York: Wiley, 1983; Moscow: Mir, 1986).
28. Danielson K.J., Baribault H., Holmes D.F., Graham H., Kadler K.E., Iozzo R.V. *J. Cell Biol*., **136**, 729 (1997).
29. Afanas'ev Yu.I., Yurina N.A., et al. *Gistologiya* (Histology) (Moscow: Meditsina, 1989).
30. Hemenger R.P. *Appl. Opt*., **28**, 4030 (1989).
31. Hemenger R.P. *J. Biomed. Opt*., **1**, 268 (1996).